JOURNAL OF MATERIALS SCIENCE 25 (1990) 3701–3708

Aluminium titanate formation by solid state reaction of Al_2O_3 and TiO_2 single crystals

B. FREUDENBERG*, A. MOCELLIN**
Laboratoire de Céramique, Ecole Polytechnique Fédérale de Lausanne, 34, Chemin de Bellerive CH – 1007 Lausanne, Switzerland

Al_2O_3 and TiO_2 reaction couples have been prepared from polished prisms of sapphire and rutile single crystals with both ***c*** axes normal to the common interface. The microstructures were analysed after heat treatments in oxygen at 1690 and 1780 K respectively, sometimes with a superimposed 20 K temperature difference across the rutile. A polycrystalline reaction layer develops via a complex nucleation and growth mechanism after an apparent incubation time during which the TiO_2 crystals saturate themselves with aluminium by Al_2O_3 dissolution and solid state transport. A quantitative evaluation of the growth kinetics also provides self-consistent estimates of effective diffusivities along the TiO_2 ***c*** axis and across the titanate layer, respectively.

1. Introduction

Previous papers [1, 2] have described Al_2TiO_5 formation in compacted Al_2O_3–TiO_2 powder mixtures with different impurity contents and particle sizes. Depending upon temperature, different overall reaction kinetics and microstructural evolutions were observed, and attributed to variations in the reaction mechanisms. In the lower temperature range, that is slightly above the Al_2TiO_5-decomposition temperature of about 1553 K [3], the small chemical driving force cannot overcome strain energy effects associated with bulk nucleation. Titanate growth can thus start only from a limited number of nucleation sites. The nucleation hindrance at lower temperatures ($\leqslant$ 1600 K) allows for the survival well into the growth stage of metastable arrangements with the phase sequence Al_2TiO_5–TiO_2–Al_2O_3. Here the TiO_2 has a double role: as reactant and as a rapid aluminium-transporting medium which allows for high growth velocities. At higher temperatures ($\geqslant$ 1700 K) rapid nucleation leads to the thermodynamically stable diffusion couple arrangement TiO_2–Al_2TiO_5–Al_2O_3. The observed low product growth velocities despite higher temperatures are thought to be due to low reactant mobilities through the Al_2TiO_5 layer, supposedly the rate-controlling step.

In this paper complementary results on the Al_2TiO_5-forming reaction are reported, based on work with macroscopic Al_2O_3 and TiO_2 single crystals. A geometric upscaling of the stable TiO_2–Al_2TiO_5–Al_2O_3 reaction couple configuration emphasizes the importance of the initial step of Al_2O_3 dissolution into TiO_2. This aspect could be neglected in powder compacts where the mean TiO_2 particle size R is small, i.e. the amount of Al_2O_3 dissolved into TiO_2 grows with R^3 and the time needed to saturate TiO_2 increases with R^2. On the other hand, the design of a macroscopic metastable Al_2TiO_5–TiO_2–Al_2O_3 couple would require a tight control over the nucleation sites at the man-made surfaces. Therefore, a temperature gradient was chosen as an alternative driving force to induce aluminium-transport across the TiO_2. Under such conditions, as for the metastable couple, a linear growth kinetic is expected, contrary to the stable couple case where the growing product layer at the Al_2O_3–TiO_2 interface is slowing down further reaction progress. So two different couple designs were chosen in order to qualitatively study the morphological evolution and transport in TiO_2 and Al_2TiO_5:

(i) isothermal Al_2O_3–TiO_2 couple; mostly showing initial dissolution of Al_2O_3 into TiO_2 due to the important aluminium solubility and mobility in TiO_2 and final Al_2TiO_5 growth at the interface.

(ii) Al_2O_3–TiO_2–Pt or Al_2O_3–TiO_2–Al_2O_3 couple exposed to a temperature gradient in which Al_2O_3 dissolves at the hot side and precipitates as Al_2TiO_5 at the cold side after transport across the TiO_2.

In the following attention will be restricted to bulk transport mechanisms since, as previously reported [2, 4], both vapour transport and surface diffusion provide only limited contributions to the overall reaction kinetics, except perhaps at high temperatures during the final stage of reaction in mixed powders.

2. Experimental procedures

The chemical analysis of the α-Al_2O_3† and TiO_2–rutile‡ single crystals is given in Table I. Making use of the Laue technique both crystals were oriented parallel to

* *Present address*: Cremer Forschungsinstitut, Oeslauer Strasse, 35, D 8633 Rödental, West Germany.
** *Present address*: Ecole des Mines, Parc de Sanrupt, F-54000-Nancy, France.
† H. Djevahirdjian, Monthey, Switzerland.
‡ Nakazumi Earth Crystals Corporation, Osaka, Japan.

0022–2461/90 $03.00 + .12

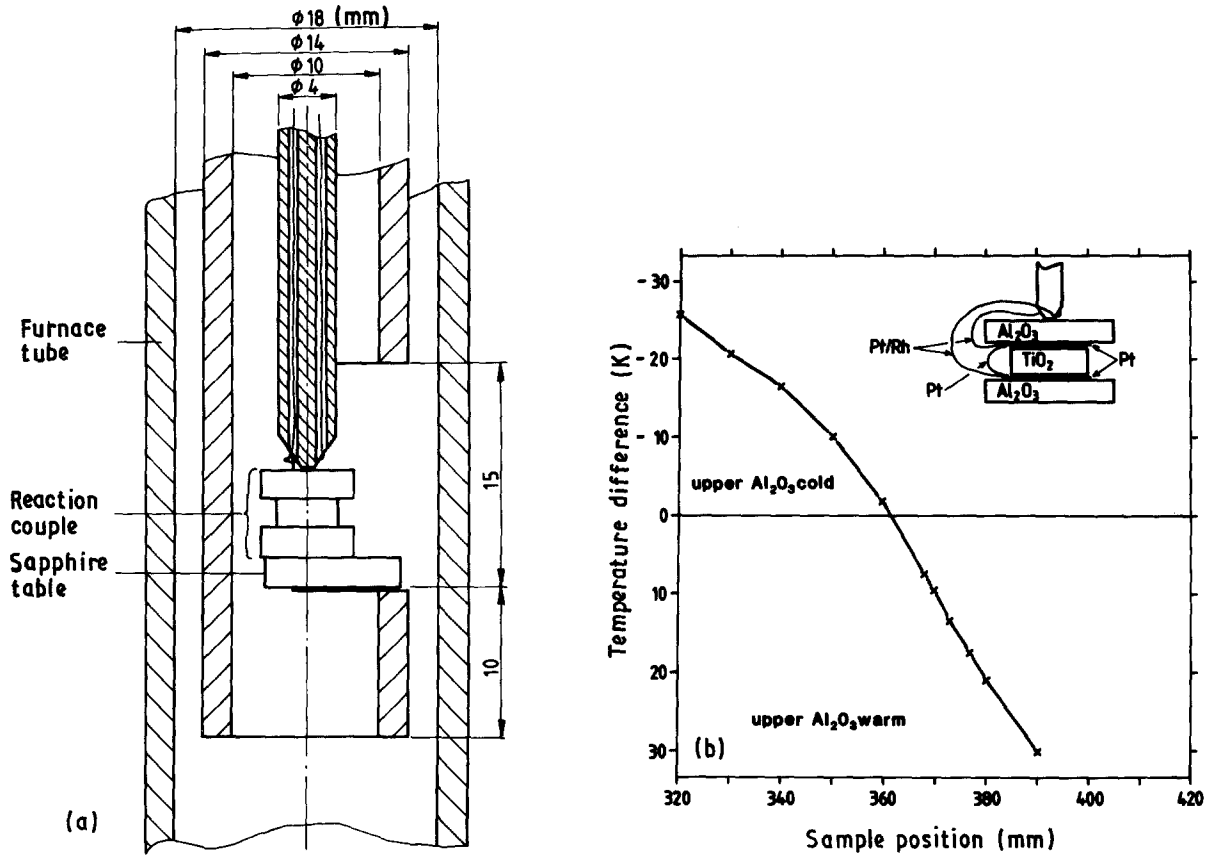

Figure 1 Couple geometry (a) Details of sample holder. (b) Temperature difference across rutile prism as a function of furnace position, $T = 1780\,K$.

their *c* axis, with their common interface normal to it. The contact face received an optical polish with a surface roughness $Ra \leqslant 0.03\,\mu m$ and a flatness better than one interference line, i.e. less than $0.3\,\mu m$. After careful cleaning in different organic solvents the couples were mounted in a high-purity alumina sample holder (Fig. 1a) applying a load of about 1 N to improve the contact.

Firing was carried out in a vertical molybdenum wound hydrogen-protected furnace*. The work tube of the furnace consisted of 99.8% alumina, flushed with upstreaming oxygen at 0.1 MPa (1 atm). The sample was exposed within 16 min. to the maximum temperature, either 1690 or 1780 K. While the reproducibility of the maximum temperature was better than $\pm 3\,K$, its absolute value at the reaction interface is known only within $\pm 15\,K$. By moving the sample holder out of the narrow homogeneous temperature zone, a temperature gradient was applied across the couple, as shown on Fig. 1b, together with the temperature difference measuring device. This effect was used to establish a temperature difference of $\Delta T = 20 \pm 7\,K$ across the rutile slice in a second type of experiment.

For the isothermal reaction, either Al_2O_3–TiO_2–Pt couples were used or, alternatively, Al_2O_3–TiO_2–Al_2O_3 couples containing two symmetrical reaction interfaces. The effective height of the TiO_2 prisms was 1.8 or 2.0 mm as measured from the Al_2O_3–TiO_2 interface to the platinum interface or the symmetry plane. The Al_2O_3 crystals were always larger ($\sim 5 \times 8\,mm^2$) than the TiO_2 crystals ($\sim 4 \times 5\,mm^2$). The grad *T* experiments were performed with Al_2O_3–TiO_2–Pt couples, Al_2O_3 and platinum at the warm and cold side, respectively, $l_{TiO_2} = 1.8 \pm 0.05\,mm$. Complementary information on nucleation and growth morphology was collected with couples where the high-purity platinum-foil at the cold side was replaced by Al_2O_3, for these couples $l_{TiO_2} = 4\,mm$.

After cooling, all samples were cracked along the interface thus requiring careful impregnation and polishing [5]. The morphological evolution was studied using optical and scanning electron microscopes† (SEM), mostly in the back-scattered electron mode. The quantitative parameters, schematically shown in Fig. 2, were measured either by SEM or by profile projector‡. X-ray diffraction measurements§ with a texture goniometer, using nickel-filtered Cu K_α radiation, yielded information on the Al_2TiO_5 crystallographic orientation with respect to the Al_2O_3 and TiO_2 single crystals. Due to the limited number of reflecting grains, the pole figures contain only isolated spots, as will be seen in Figs 7b and 9.

3. Results and discussion

3.1. Isothermal reaction couple

3.1.1. Microstructural evolution

A complex microstructural evolution is observed in

*PCA 10/10 Metals Research, Cambridge, UK.
†S100 and S250, Cambridge Instruments Ltd, Royston, Herts, UK.
‡M129, Isoma, Bienne, Switzerland.
§D500, Siemens, Karlsruhe, Federal Republic of Germany.

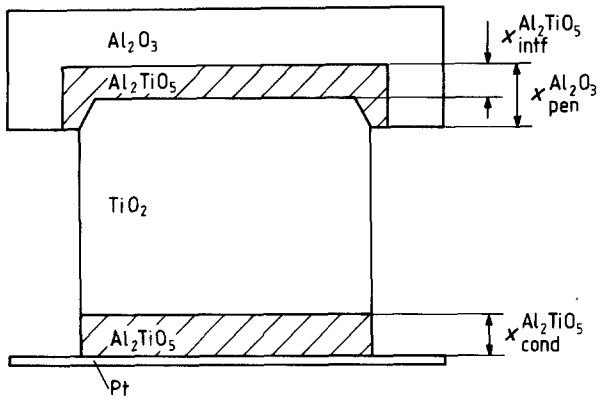

Figure 2 Schematic view of the reaction couple showing the measured parameters.

TABLE I Single crystal chemical analysis

	α-Al_2O_3 (p.p.m. weight)	TiO_2-rutile (p.p.m. weight)
Na_2O	50*	10
K_2O	n.d.*	10
MgO	n.d.	n.d.
CaO	n.d.	n.d.
Al_2O_3	–	100*
Ga_2O_3	n.d.	–
TiO_2	150	–
SiO_2	100	n.d.
SnO_2	n.d.	n.d.
Nb_2O_5	–	n.d.
Fe_2O_3	n.d.	n.d.
MnO	n.d.	n.d.

*Neutron activation analysis by Dr J.-D. Fridez; all other data from the Federal Laboratories for Materials Testing and Research, Dübendorf, Switzerland;
n.d.: not detected.

the isothermal couples. Three different stages may be identified (Fig. 3). During the initial stage the rapid penetration of TiO_2 into the dissolving Al_2O_3 crystal is accompanied by a pronounced interface instability. The intermediate stage shows a certain smoothing of the interface now covered by a detectable Al_2TiO_5 layer. During the final stage a continuous layer of aluminium titanate evolves without further dissolution into the TiO_2 detectable.

Initially, the as-polished Al_2O_3- and TiO_2-surfaces with a roughness $R_a \leqslant 0.03\,\mu m$ enter only locally into a solid–solid contact. At these points aluminium dissolution into the TiO_2 takes place [6, 7]. An aluminium-enriched TiO_2 region thus gradually grows in the vicinity of every initial Al_2O_3–TiO_2 contact and at the expense of the sapphire phase. TiO_2 protrusions and Al_2O_3 cavities more or less reminiscent of those found [8] during $NiAl_2O_4$ growth on Al_2O_3 surfaces, subsequently grow more regularly in the interface region (Fig. 3a). The detailed geometry of such protrusions apparently alternating with voids would deserve further investigation as it may be due to several different effects including surface energy driven instabilities or solute redistribution possibly affected by local stress due to molar volume changes. It is nonetheless worth pointing out that no correlation was found between such geometry and the initial topography of the reacting crystals.

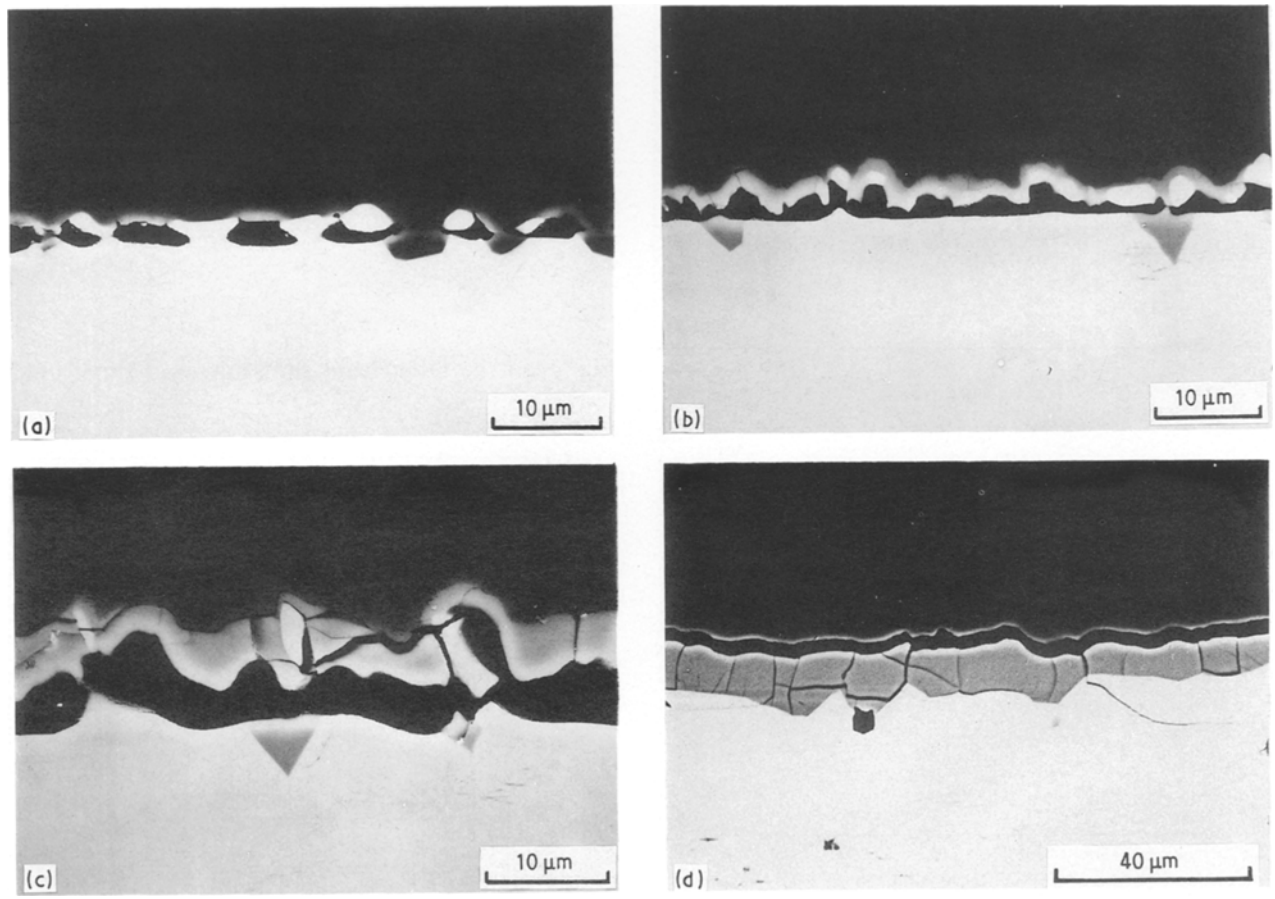

Figure 3 Isothermal reaction couple (white: TiO_2, grey: Al_2TiO_5, dark grey: Al_2O_3) (a) 3 h at 1690 K, l_{TiO_2} = 1.0 mm, initial stage; (b) 10 h at 1780 K, l_{TiO_2} = 2.0 mm, intermediate stage; (c) 30 h at 1690 K, l_{TiO_2} = 1.0 mm, intermediate stage; (d) 60 h at 1780 K, l_{TiO_2} = 1.8 mm, final stage.

Later on, or after the same period of time but at higher temperature, the rate of dissolution slows down, and an Al_2TiO_5 layer, about 1 μm thick, is detected by SEM in the back scattered mode (Fig. 3b). Such a thickness corresponds roughly to the limit of detection which varies also depending on the local geometry. The protrusions become progressively pinched off, sometimes leaving a TiO_2-droplet in the cavity. It is generally observed that the Al_2TiO_5 crystals grow on the Al_2O_3 side of the gap (Fig. 3c). Finally, the appearance of the aluminium titanate layer becomes more regular. Once the product layer attains a thickness of about 10 μm, most of the pores have been eliminated, with a few exceptions at the Al_2TiO_5–TiO_2 side (Fig. 3d). Upon further observation of the Al_2O_3–Al_2TiO_5 and Al_2TiO_5–TiO_2 interfaces, the former shows an apparent waviness while the latter exhibits facets and structures recalling grain-boundary grooves. They suggest an Al_2TiO_5 lateral grain length between ≈ 10 and ≈ 50 μm. These features do not change significantly between 10 and 300 h of reaction time at 1780 K. Evidence from texture analyses presented below reveals a statistical orientation of the Al_2TiO_5 grains. And the rather uniform thickness of the Al_2TiO_5 layer does not point to preferential transport across certain grains or grain boundaries.

In the end, i.e. after the couples are brought back to room temperature, except for a border zone 10 to 100 μm thick, the rutile is dotted all over with precipitates rich in aluminium as evidenced by microprobe analysis (Fig. 3d, bottom and Fig. 8 below). According to Thong *et al.* [9], these are oriented Al_2O_3 crystals. They form on cooling when the TiO_2 becomes supersaturated in aluminium, thus explaining why our microprobe detected only about 2 cat. % aluminium dissolved in the precipitate free zone of rutile whereas literature [10] reports aluminium solubilities reaching 3 to 4 cat. % in rutile at 1690 K. Using the diffusion coefficient as estimated below for aluminium in TiO_2, and the solution to Fick's equation for a finite slab [11], the time needed to drain 1 cat. % aluminium out of the border zone 50 μm thick can be estimated to reach from ~ 1 to ~ 10 min at fixed temperatures from 1700 to 1500 K respectively. Considering as realistic an initial cooling rate of $\sim 50\,K\,min^{-1}$ at the couple interface region, the precipitate free zone appears to reflect aluminium drainage toward the free TiO_2 surface or the Al_2TiO_5 layer during cooling, thus consistent with the proposed interpretation [9]. The absence of a precipitate free zone around cracks as seen in Fig. 6 below suggests that they have formed on cooling.

3.1.2. Overall dissolution and growth kinetics

While the description of the microstructural evolution remained mostly qualitative, an approximate quantification of the overall reaction kinetics may be attempted through directly measurable parameters (Fig. 2): the penetration depth of rutile into Al_2O_3, and the thickness of the Al_2TiO_5 layer formed at the interface respectively. Figs 4a and 4b show the time variation of the amount of Al_2O_3 dissolved into the TiO_2 slab at 1690 and 1780 K respectively, as an effective thickness $x_{diss}^{Al_2O_3}$ along the TiO_2 *c* axis. The plotted data points were obtained from straight penetration depths $x_{pen}^{Al_2O_3}$ measured on polished micrographs and corrected for more or less concurrent Al_2TiO_5 layer growth via the relation

$$x_{diss}^{Al_2O_3} = x_{pen}^{Al_2O_3} - 0.52\, x_{intf}^{Al_2TiO_5} \quad (1)$$

Fig. 5 on the other hand shows an isothermal time

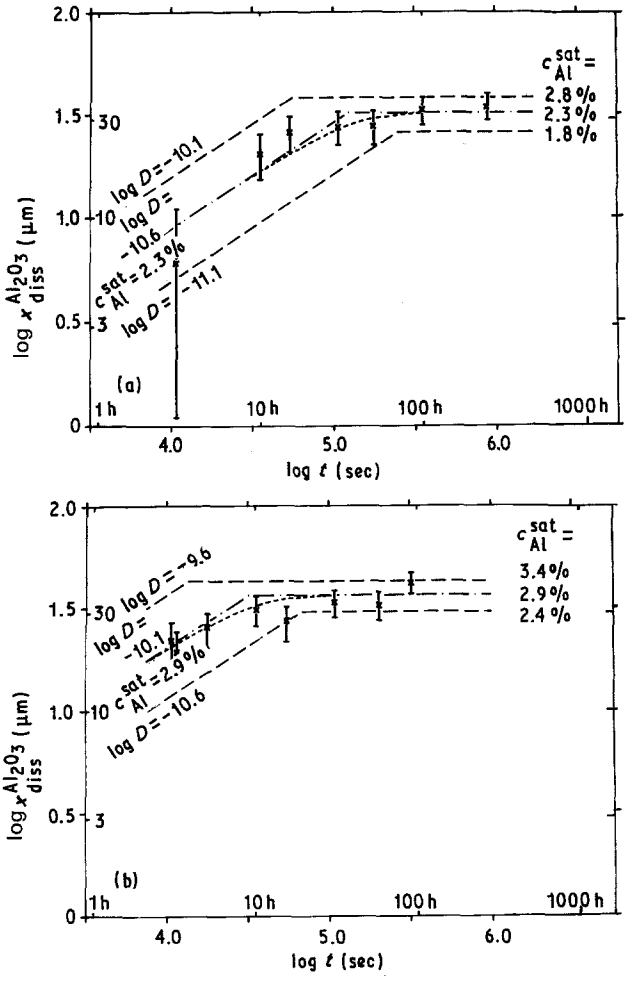

Figure 4 Isothermal reaction couple (a) Al_2O_3 dissolution kinetic at 1690 K, l_{TiO_2} = 2.0 mm; (b) Al_2O_3 dissolution kinetic at 1780 K, l_{TiO_2} = 1.8 to 2.0 mm.

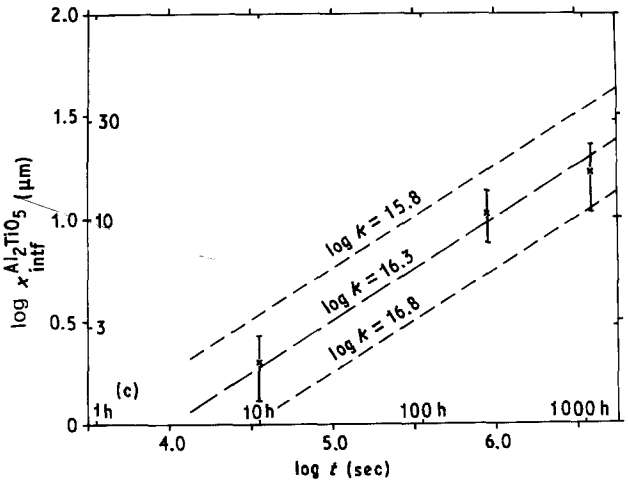

Figure 5 Isothermal reaction couple, Al_2TiO_5 growth kinetic after rutile saturation at 1690 K.

TABLE II Isothermal aluminium dissolution and Al_2TiO_5 growth parameters

Temperature (K)	Aluminium solubility limit in TiO_2 (cat. %)	Effective aluminium diffusivity TiO_2 *c* axis ($m^2 sec^{-1}$)	Al_2TiO_5 parabolic growth rate constant ($m^2 sec^{-1}$)
1690	2.3 ± 0.5	$10^{-10.6\pm0.5}$	$10^{-16.3\pm0.5}$
1780	2.9 ± 0.5	$10^{-10.1\pm0.5}$	$10^{-15.5\pm1.0}$

dependence of the average Al_2TiO_5 layer thickness at long reaction times, i.e. after the starting TiO_2 crystal may be considered to have been saturated with aluminium so that only Al_2TiO_5 formation is taking place in the system.

At small times, i.e. far from saturation, dissolution proceeds according to [11, p. 61, equation (11) integrated]:

$$m_A(t) = 2C_{Al}^{sat}\left(\frac{D}{\pi}\right)^{1/2} t^{1/2} \quad (2)$$

where D is the effective diffusion coefficient ($m^2 sec^{-1}$), t the time (sec), C_{Al}^{sat} the cation-concentration at saturation ($\%\frac{Al}{Al+Ti}$), m_A the dissolved amount per area (% m). The final plateau on Fig. 4 directly gives the saturation concentration C_{Al}^{sat} in ($\%\frac{Al}{Al+Ti}$) knowing that 1 μm of Al_2O_3 dissolved gives an aluminium concentration of 0.143 cat. % for each 1 mm thickness of TiO_2 slab. Also, from the initial slopes of Fig. 4 numerical values for the product $C_{Al}^{sat} D^{1/2}$ may be extracted assuming Equation 2 to hold (i.e. no interface reaction control of the process). Therefore the effective diffusivity D of aluminium along the TiO_2 *c* axis may be estimated. The corresponding evaluations are collected together in Table II, with values for the Al_2TiO_5 growth rate constant k obtained from Fig. 5 and under the hypothesis of parabolic kinetics

$$(X_{intf}^{Al_2TiO_5})^2 = 2kt \quad (3)$$

which are usually found to occur when diffusion across the product phase is rate-controlling. Obviously, the accuracy of such estimates cannot be very high, given the simplifying assumptions on which they are based and the experimental error due to the perturbated interfaces. They nonetheless are thought to provide realistic orders of magnitude.

Finally, electron microprobe measurements of aluminium and titanium concentrations respectively in the aluminium titanate phase could be made with sufficient precision to detect small concentration gradients across the product layer: $|\Delta C\ Al_2O_3| \approx |\Delta C\ TiO_2| \approx 0.5 \pm 0.2$ wt % at 1780 K.

It has been shown elsewhere [5] that for the hypothetical case of cation counter diffusion in Al_2TiO_5 the aluminium-flux is related to the concentration gradient and the diffusion coefficient D_{slow} representing the slowest, i.e. rate-controlling cation, by

$$J_{Al} = -2(\pm 0.2) D_{slow} \frac{\Delta C_{Al}}{\Delta x} \quad (4)$$

where $\log J_{Al} = -6.3 \pm 1\ mol_{Al} m^{-2} sec^{-1}$ as obtained from $\log k = -15.5 \pm 1\ m^2 sec^{-1}$ and $\Delta x = 10^{-5}$ m, $\Delta C_{Al} = 350 \pm 150\ mol_{Al} m^{-3}$, a value for D_{slow} is computed at 1780 K, $\log D_{slow} = -14.2 \pm 1.5\ m^2 sec^{-1}$. This is of the order of four orders of magnitude smaller than the aluminium diffusivity into TiO_2, see Table II, thus confirming the initial dominating influence of aluminium dissolution over the reaction *per se*.

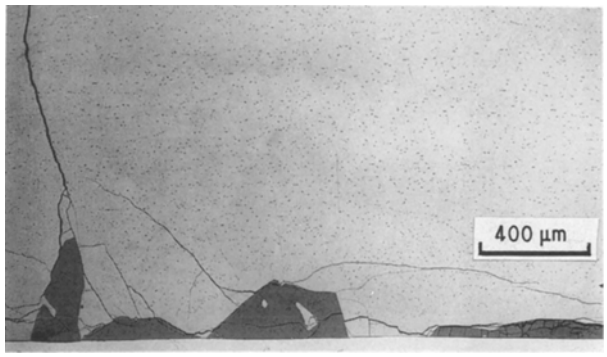

Figure 6 Reaction couple under thermal gradient, 180 h at 1780 K, ΔT = 20 K, Al_2TiO_5 condensation on platinum foil at the cold side.

3.2. Reaction couple under thermal gradient

3.2.1. Microstructural evolution

As previously mentioned in a second type of experiment, a temperature difference $\Delta T = 20 \pm 7$ K was imposed on the TiO_2 part of the reacting couples whereas the mean temperature was kept at 1780 ± 15 K. At the hot end of the couple, during the rapid initial aluminium dissolution the same Al_2O_3–TiO_2 interface instabilities were observed as for the isothermal couples. Later a thin corrugated Al_2TiO_5 layer appeared. However, due to the continuous withdrawal of aluminium, the titanate layer never grew beyond a mean thickness of about 6 μm. At the cold side, on the platinum layer, isolated facetted Al_2TiO_5 crystals, sometimes containing TiO_2 inclusions, grew after saturation of the rutile matrix. A cut parallel to the aluminium and heat-flux is shown on Fig. 6, while Fig. 7 provides an example of a cut normal to the flux after removal of the platinum layer. The mean centre-to-centre distance of the Al_2TiO_5 islands is about 500 μm. Systematic X-ray texture analyses of those islands were performed and Fig. 7b shows a stereographic plot of the (200) Al_2TiO_5 line orientations from a typical sampling such as illustrated on Fig. 7a. The absence of any preferential orientational relation between Al_2TiO_5 crystals and TiO_2 suggests a weak interaction between both lattices during nucleation, the latter representing a difficult step as demonstrated by the scarcity of growth sites. The specific reasons controlling the spacing between the islands or the polyhedral form of the precipitates have not been identified.

In a complementary set of experiments the platinum layer at the cooler side of the rutile was replaced by a sapphire crystal (Fig. 8). Initially, both the cold and the warm interfaces showed the same instability associated with the rapid dissolution. After about 3 h a thin primary Al_2TiO_5 layer forms at both interfaces. Once saturation of the bulk TiO_2 has been achieved, a

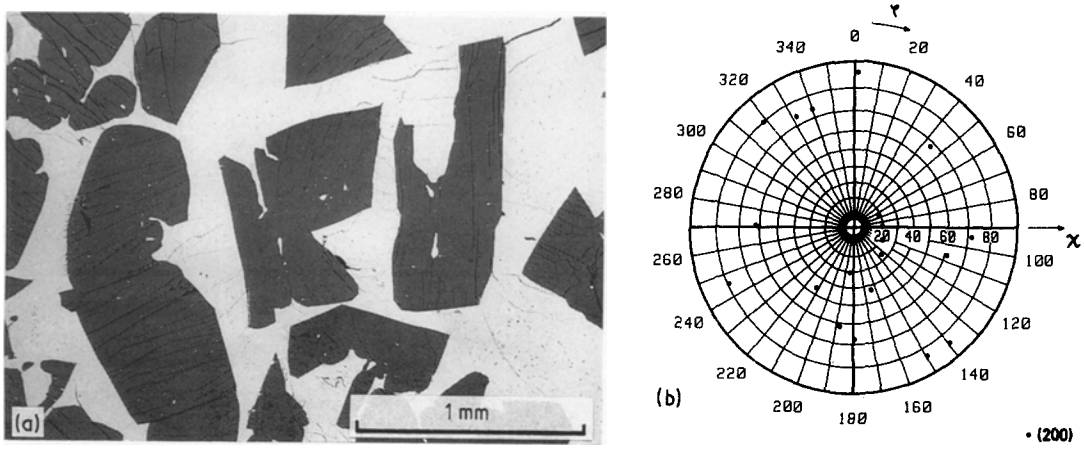

Figure 7 (a) Reaction couple under thermal gradient, 91 h at 1780 K, Al_2TiO_5 islands condensed on platinum foil, seen from below after removal of platinum; (b) Texture analysis of the Al_2TiO_5 islands shown in Fig. 7a; the macroscopic flux is oriented normal to the drawing, Al_2TiO_5 (200) reflection.

secondary Al_2TiO_5 layer starts to condense on the cold side. A row of pores is trapped between primary and secondary aluminium titanate, serving as natural markers. Their position indicates that the secondary titanate grows into the TiO_2, presumably bearing some orientational relationship with the underlying primary Al_2TiO_5 layer. Since the latter consists of randomly oriented crystals, as confirmed by texture analyses (Fig. 9), so does the former.

The growth front of the secondary Al_2TiO_5 on the other hand, is characterized by an increasing ruggedness which increases with time and develops into more or less well defined facets. The origin of such facets could be due to crystallographic anisotropies and include local stress field effects thus selecting preferential growth directions. But they could also arise to some extent from capillary instability of the overall Al_2TiO_5–TiO_2 interface.

3.2.2. Overall dissolution and condensation kinetics

The onset of precipitation or the end of TiO_2 saturation with aluminium can be extrapolated from the linear precipitate growth kinetic (Fig. 10) as $t_{sat} \approx 22$ h at 1780 K. The aluminium solubility difference in rutile which corresponds to a temperature difference of 20 K is approximately equal to $\Delta C_{Al}^{sat} = 0.2$ cat. % (our data and Slepetys *et al.* [10]) from the high to low temperature interface respectively. Making use of the solution to Fick's equation for a slab of finite thickness for constant diffusivity D again [11] allows D to be estimated by iteration. An effective value of $D_{Al} = 10^{-10.3\pm0.5}\,m^2\,sec^{-1}$ is found in good agreement with that evaluated above under isothermal conditions, $D_{Al} = 10^{-10.1\pm0.5}\,m^2 sec^{-1}$, thus suggesting a value of $D_{Al} = 10^{-10.2}\,m^2\,sec^{-1}$ for further calculations. This result is in good agreement with data extrapolated from Yan *et al.* [12] measurements on niobium-doped polycrystalline rutile.

When saturation has been achieved, a constant growth velocity of the condensing Al_2TiO_5 is found, $\Delta x_{cond}^{Al_2TiO_5}/\Delta t = 2.0(\pm0.2) \times 10^{-10}\,m\,sec^{-1}$ (Fig. 10), corresponding to an effective flux of aluminium ions $J_{Al} = 8(\pm1) \times 10^6\,mol\,m^{-2}\,sec^{-1}$. This flux *a priori* results from two contributions:

(i) an isothermal Fickian flux:

$$J_{Al}^{Fick} = -D_{Al}^{TiO_2}\frac{\Delta C_{Al}^{sat}}{l_{TiO_2}} \quad (5)$$

where l_{TiO_2} is the thickness of the rutile single crystal

(ii) a thermal gradient induced flux (Soret effect) [13]

$$J_{Al}^{Soret} = -D_{Al}^{TiO_2}\frac{Q_{Al}^{eff}C_{Al}}{RT^2}\frac{\Delta T}{l_{TiO_2}} \quad (6)$$

where Q^{eff} is the effective heat of transport (kJ mol^{-1}).

The flux resulting from the Fick contribution can be calculated from the available data: $J_{Al}^{Fick} \approx 4.5(\pm2.5) \times 10^{-6}\,mol\,m^{-2}\,sec^{-1}$. Comparing with the actually measured total flux, $J_{Al}^{total} = 8(\pm1) \times$

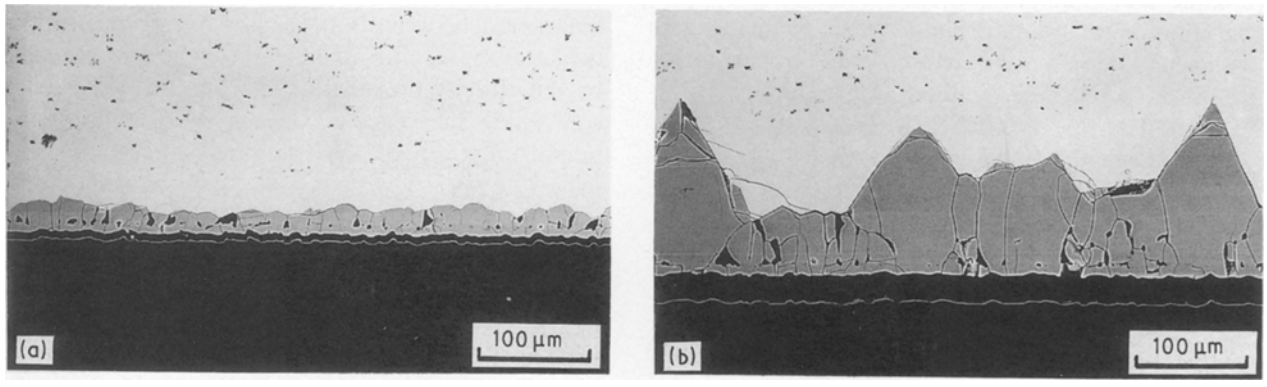

Figure 8 Reaction couple under thermal gradient; Al_2TiO_5 condensation without platinum foil (a) 30 h at 1780 K. (b) 100 h at 1780 K.

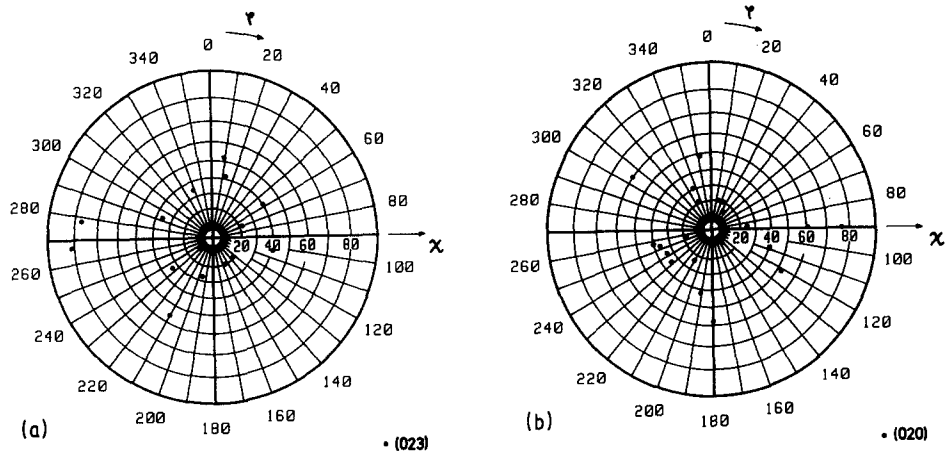

Figure 9 Texture analysis of the Al_2TiO_5 layer shown in Fig. 8b after removal of the sapphire crystal; the macroscopic flux is oriented normal to the drawing (a) Al_2TiO_5 reflection (023), (b) Al_2TiO_5 reflection (020).

10^{-6} mol m^{-2} sec^{-1}, we find that the additive contribution by the Soret effect, J_{Al}^{Soret} lies somewhere between 0 and the same order of magnitude as the Fick term, corresponding to an effective heat of transport $0 \leqslant Q_{Al}^{eff} \leqslant 200\,kJ\,mol^{-1}$. Such a range for a heat of transport appears to be a rather common finding for solid oxides [13, 14].

Under stationary dissolution-condensation conditions, a constant mean titanate layer thickness at the hot interface is found: $x_{intf}^{Al_2TiO_5} = 5.5(\pm 2)\,\mu m$ (Fig. 10). The titanate layer is in fact migrating, "digesting" Al_2O_3 at the warm side and "exuding" it into TiO_2 thus supplying the aluminium-flux toward the cold side. If the net flux across the titanate layer is diffusion controlled, as was already assumed previously, then [15]

$$\frac{\Delta x_{cond}^{Al_2TiO_5}}{\Delta t} = \frac{k}{x_{intf}^{Al_2TiO_5}} \qquad (7)$$

where k is the growth rate constant for Al_2TiO_5 formation (m^2 sec^{-1}).

Here the amount of Al_2TiO_5 formed does not stick to the product layer at the warm interface but is the increase of the condensed layer. Given the condensation velocity and the thickness of the product layer, a parabolic growth rate constant can be found: log $k = -15.0(\pm 0.5)$ (m^2 sec^{-1}) at 1780 K. This value is again in good agreement with that found under isothermal conditions (Table II).

4. Conclusion

The present work which has dealt with macroscopic single crystal reaction couples submitted to two different kinds of heat treatment is believed to yield the following main conclusions

(i) An initial rapid dissolution of Al_2O_3 into TiO_2 takes place prior to the observable beginning of the Al_2TiO_5 forming reaction, together with the development of significant interfacial shape instabilities.

(ii) The formation of the aluminium titanate product phase subsequently occurs in a complex geometrical environment. The physical nature of the limited number of easy-to-nucleate sites has not been identified. Obviously these sites are without any orientational relation to their substrates.

(iii) Upon prolonged reaction a continuous polycrystalline layer results in isothermal couples with a roughly uniform thickness at long distance but locally undulated. Conversely, an amplifying waviness is observed in the reaction couples exposed to a temperature gradient.

(iv) Assuming the observed phenomena to be kinetically controlled by diffusion in the solid state, effective diffusivities across TiO_2 and Al_2TiO_5 respectively can be estimated which are consistent with already published values from independent experimental arrangements.

More generally, considering the present and previous studies [1, 2] together, it is clear that much

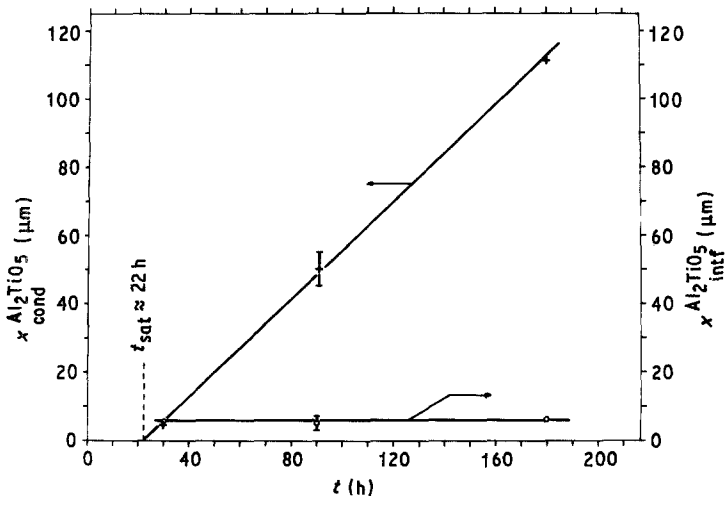

Figure 10 Reaction couple under thermal gradient at 1780 K, $\Delta T = 20$ K; Al_2TiO_5 condensation kinetic and Al_2TiO_5 thickness at the warm Al_2O_3/TiO_2 interface.

more systematic work would still be necessary, focused in particular on crystallographic anisotropies and local stress effects before the $Al_2O_3 + TiO_2$ reaction mechanism is well understood. However, it is also clear that whatever the geometry, i.e. single crystals or powders, the rutile phase plays the peculiar role of being both a reacting and aluminium-reactant transporting phase, whereas Al_2TiO_5 acts as a diffusion barrier as is more classical of the product phase in solid state reactions. Finally, it appears interesting to note that the flux of aluminium across TiO_2 induced by a temperature gradient across the rutile may be readily observed at a magnitude comparable to those fluxes encountered in isothermal reactions driven by a chemical potential gradient only.

Acknowledgements

Help from Mr G. Burri for electron probe microanalysis is gratefully acknowledged.

References

1. B. FREUDENBERG and A. MOCELLIN, *J. Amer. Ceram. Soc.* **70** (1987) 33.
2. *Idem., ibid.* **71** (1988) 22.
3. E. KATO, K. DAIMON and J. TAKAHASHI, *ibid.* **63** (1980) 355.
4. B. FREUDENBERG and A. MOCELLIN, 2nd International Symposium on "Ceramic Materials and Components for Engines", Lübeck-Travemünde, FRG, April 14-17, 1986, pp. 381-387.
5. B. FREUDENBERG, Thesis no. 709, Ecole Polytechnique Fédérale de Lausanne (1987).
6. K. HOSHINO, N. L. PETERSON and C. L. WILEY, *J. Phys. Chem. Solids* **46** (1985) 1397.
7. J. SASAKI, N. L. PETERSON and K. HOSHINO, *J. Phys. Chem. Solids* **46** (1985) 1267.
8. Y. K. SIMPSON and C. B. CARTER, *Phil. Mag.* **53A** (1986) L1.
9. N. THONG, C. CARRY and P.MOECKLI, *J. Amer. Ceram. Soc.* **66** (1983) C-225.
10. R. A. SLEPETYS and P. A. VAUGHAN, *J. Phys. Chem.* **73** (1969) 2157.
11. H. S. CARSLAW and J. C. JAEGER, in "Conduction of Heat in Solids", 2nd ed. (Clarendon Press, Oxford, 1984).
12. M. F. YAN and W. W. RHODES, *J. Apply. Phys.* **53** (1982) 8809.
13. F. A. NICHOLS, G. P. MARINO and H. OCKEN, in "Mass Transport Phenomena in Ceramics", edited by A. R. Cooper and A. H. Heuer. Mater. Sci. Research Vol. 9, 1975, Plenum Press, N.Y., pp. 75-96.
14. H. REUTHER, J. WIEGMANN and W. HINZ, *Glastechn. Berichte* **56** (1983) 19.
15. W. JANDER, *Zeit. Anorgan. Allg. Chemie* **163** (1927) 1.

Received 21 February
and accepted 30 August 1989